Electromechanical Energy Conversion Systems (EECS)
Niroo Research Institute (NRI)
Vol. 4, No. 2, Summer 2025, pp. 1- 7
DOI: 10.30503/EECS.2025.488460.1064
Original Article

Machine Learning Ball-Bearing Fault Detection Methods Using Envelope Analysis and Power Spectral Density

Mohammad Hatami Kakesh[1], Akbar Rahideh[1*], Gholam Rezah Agah[1], and Shahin Hedayati Kia[2]

Abstract

Ball-bearings are one of the most important components in rotating machinery. Due to the practical importance of rotating machineries in industry, fault detection has become inevitable. Various techniques have been implemented for ball-bearing fault detection using vibration signals. In this research, vibration signal analysis methods are presented to extract suitable features for training some of the machine learning techniques in order to diagnose ball-bearing defects in different speeds. The purpose of this study is to obtain a highly accurate algorithm and compare its performance with that of other machine learning algorithms. To achieve this goal, Hilbert transform has been applied for envelope analysis to attenuate the frequencies that are not related to ball-bearing fault and perform power spectral density and descriptive statistics to extract features. Also comparison and evaluation of random forest, support vector machine, artificial neural network and k-nearest neighbour have been carried out for this study. For a dataset with 1465 samples in various speed, random forest has achieved an accuracy of above 97%.

Keywords: Fault Detection, Ball-bearing, Machine learning, Signal Processing, Induction Motor.

Received Date: 2024-11-12; Revised Date: 2025-03-18; Accepted Date: 2025-08-13

1. INTRODUCTION

Nowadays, electrical machines are widely used in applications such as pump, fan, etc. in industrial, domestic and commercial sectors [1]. Induction motors due to their simple structure, high reliability, longer lifetime and uncomplicated maintenance are among the best options when both performance and economic factors are important [2-5]. However, factors such as frequent start and stop, working under various operation conditions, contaminated environment and uninterrupted working can cause deterioration in motor performance and occurrence of fault. If the fault is not detected at early stage, the complete shutdown and unexpected breakdown of motor is possible to happen and causes an irreparable damage to the production system [5], [6]. Therefore, fault detection in induction motors has become a necessary and important task to prevent unexpected failures. Maintenance strategies are divided into three categories: (1) reactive maintenance in which motors operate until their failure; (2) preventive maintenance in which motors are checked at regular time intervals and essential repairs are carried out in case of any detected fault; and (3) predictive maintenance which requires continuous condition monitoring and recommends action based on the collected information during condition monitoring [7]. The main induction motor failures can be classified into the broken rotor bar, stator winding short circuit, eccentricity and bearing faults. Many reports show that above %40 of induction motors defects are related to bearing faults. Ball-bearings are one of the most essential components that help motors moving smoothly and also reduce friction. Therefore, ball-bearing fault detection has become essential [8], [9]. Fault diagnosis of rotating machinery can be classified into signal based and model based methods. Signal based methods using signal processing approaches in the time domain, frequency domain and time-frequency domain are applied to diagnose the motor faults. Techniques like fast Fourier transform (FFT), power spectral density (PSD), short time Fourier transform (STFT), empirical mode decomposition (EMD), ensemble empirical mode decomposition (EEMD), variational mode decomposition (VMD), Hilbert Huang transform (HHT), wavelet transformation (WT) and wavelet pocket transformation (WPT) have been applied for detecting the fault of motors [10-14]. Recently, with remarkable progress of technologies and increase in data volume, application of machine learning and artificial intelligence methods has been highly welcomed to boost

[1] *Department of Electrical Engineering, Shiraz University of Technology*
[2] *Université de Picardie JulesVerne, 80039 Amiens, France*
**Corresponding author: rahideh@sutech.ac.ir*

productivity in various fields. Thus, ball-bearing fault detection using machine learning approaches attracted researcher's attention. Support vector machines (SVM) [15], [16], artificial neural network (ANN) [17], [18], random forest (RF) and k-nearest neighbor (KNN) [19], [20] can be named as the most popular machine learning algorithms. Extracting appropriate features are significantly influential on the accuracy and efficacy of the method. Consequently, many studies have focused on machine learning and signal processing combined methods [14], [21]. In this study, a procedure is proposed for accurate ball-bearing fault detection method using vibration signal. The contribution and novelty of the proposed method is due to proper sequence and arrangement of the employed signal processing and machine learning methods. For this task, the Hilbert transform is used to obtain envelope of the signal to amplify the fault frequency characteristics and attenuate the frequencies that are not related to the bearing fault. Both Hilbert transform and its power spectral density are used to extract the features in both time and frequency domains.

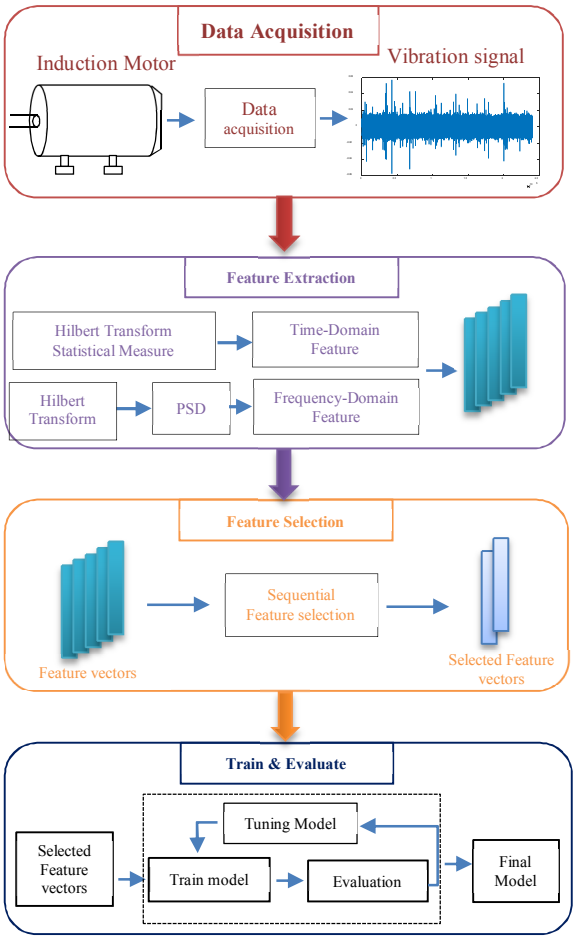

Fig. 1. Flowchart of the proposed method

The most informative features in both time and frequency domains are selected using sequential feature selection method. These features are used to train four different machine learning methods, i.e. random forest, support vector machine, artificial neural network and k-nearest neighbor. The performances of these four machine learning methods are compared in terms of various criteria. While traditional signal processing techniques can extract important features, combining these features with machine learning algorithms enables the identification of more complex and nonlinear patterns that may not be detectable by traditional methods. In the next section, the proposed method for ball-bearing fault detection using signal processing and machine learning is presented.

2. Methodology

2.1. Proposed Method

The flowchart of the proposed method is shown in Fig. 1. First, the vibration signal is obtained via the installed vibration sensor on the squirrel-cage induction motor. Second, by utilizing the Hilbert transform on the raw vibration signal, the envelope of the signal is acquired and the time domain features are extracted using descriptive statistics. Then, PSD is applied on the signal envelope and the statistical features are computed on the predefined range around the fault frequencies to extract the frequency domain features. Afterwards, the features are normalized and the best features are chosen using the sequential feature selection to increase accuracy and reduce complexity. Lastly, the model is trained with the selected features and after tuning the model, the final model is extracted.

2.2. Machine Learning Techniques

In this subsection, some of the well-known supervised learning algorithms such as the support vector machine, K-nearest neighbor, artificial neural network and ensemble learning are briefly explained.

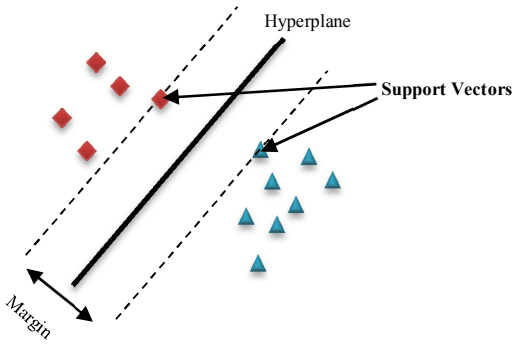

Fig. 2. A support vector machine

2.2.1. Support Vector Machine

SVM is one of the supervised learning algorithms with high accuracy and widely used in various fields. In SVM algorithm, a hyperplane is obtained during the training process to maximize the margin between the two classes [22], [23]. The SVM optimal separator hyperplane with maximum margin is defined in (1):

$$\min \frac{1}{2}\omega^T\omega + C\sum_{i=1}^{k}\zeta_i \quad (1)$$

subject to

$$y_i\left((\omega,\phi(x_i)) - b\right) \geq 1-\zeta_i\,,\zeta_i \geq 0\,,i = 1,2,\ldots,k$$

where C is the penalty parameter, ζ_i is the feature samples, ω is the weight vector, k is the number of samples, $\phi(x_i)$ is the feature mapping function, x_i is the input data points, y_i is the class label for input data point and b is the bias. A support vector machine hyperplane is illustratively shown in Fig. 2.

2.2.2. K-Nearest Neighbor

One of the simplest and yet most commonly used supervised learning methods, which is in the category of classification and regression, is the k-nearest neighbor method. This technique is a sample based algorithm in which the value of k that represents the number of neighbors is selected first. Then, the distance of each test sample and training data is calculated. Next, the k samples that have the closest distance to the test data are chosen. One of the most famous distance criteria in the KNN method is the Euclidean distance. The expression of Euclidean distance between x_i and y_i is shown in equation (2):

$$D = \sqrt{\sum_{i=1}^{l}(x_i - y_i)^2} \quad (2)$$

where D is the Euclidean distance between x_i and y_i, $x_i = [x_1 \;\; x_2 \;\; \cdots \;\; x_l]$ and $y_i = [y_1 \;\; y_2 \;\; \cdots \;\; y_l]$ are two vectors of data points in l-dimensional space. A KNN with 3 neighbors for binary classes is shown in Fig. 3.

2.2.3. Artificial Neural Network

ANN is one of the most widely used supervised algorithm, which is utilized in classification problems and pattern recognition, whose model is inspired from functioning of human brain.

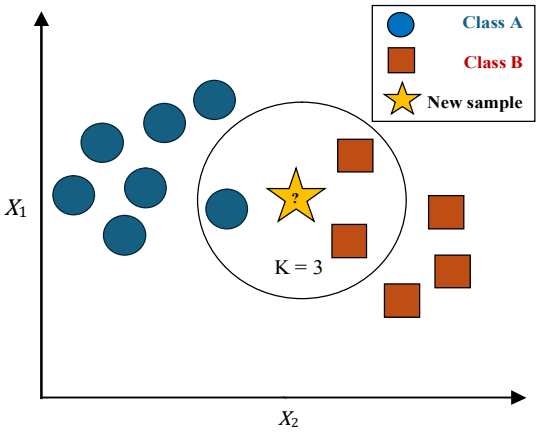

Fig. 3. A K-nearest neighbor classifier with 3 neighbors

This algorithm consists of interconnected processing units called neurons. Fig. 4 shows a neuron with N inputs. The output of the neuron is obtained according to the following expression:

$$y = f(W^TX + b) = f(\sum_{i=1}^{N} w_i x_i + b) \quad (3)$$

where $W = [w_1 \;\; w_2 \;\; \cdots \;\; w_N]^T$ is the neuron weight vector, $X = [x_1 \;\; x_2 \;\; \cdots \;\; x_N]^T$ is the neuron input vector, N is the number of inputs, b is the bias, f is the activation function and y is neuron output.

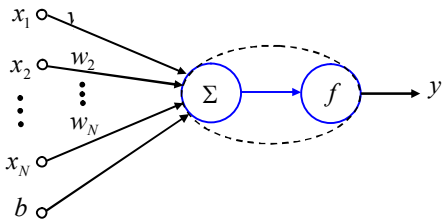

Fig. 4. A neuron with n inputs

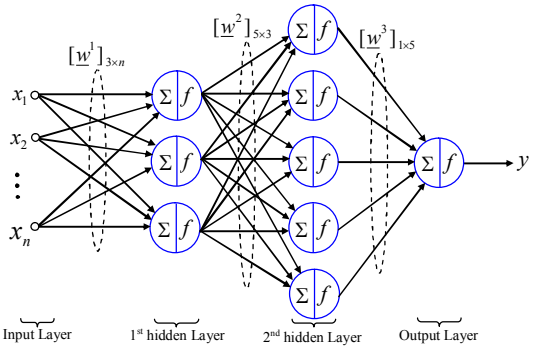

Fig. 5. A typical MLP network with n inputs and three layers

The general structure of an artificial neural network is constructed from input, output and hidden layers. Each connection between neurons has a weight adjusted during training process. A typical multi-layer perceptron (MLP)

neural network is shown in Fig. 5. Note that the biases are not shown in Fig. 5.

2.2.4. Ensemble Learning

The decision tree is one of the popular supervised machine learning algorithms that is frequently used in classification and regression cases. Each node in this tree makes a decision based on the selected feature, and branches transmit the outcome of that decision to another node. This algorithm is sensitive to slight changes in training dataset, which may cause over-fitting and the results may change significantly. To increase accuracy and performance of the model and reduce over-fitting, several machine learning models are compounded and the final output is obtained by combining individual models prediction, which is known as the ensemble learning. The random forest is a model based on the ensemble learning, which is made of several decision trees and has higher accuracy over the decision tree.

2.3. Data Acquisition

In this study, the dataset in [24] is utilized. The samples of the vibration signal were obtained from the installed vibration sensors in the radial-vertical and axial directions for the healthy state and defects of inner ring, outer ring and ball in different severities and 50, 70 and 100% of nominal speed. The implemented motor in this experiment is an 11 kW 4-pole induction motor with the rated speed of 1470 rpm and ball bearing model of 6309-C4. Each set of data is recorded for 12 seconds with the sampling frequency of 20 kHz. The laboratory system used is shown in Fig. 6. The applied ball-bearing has a pitch diameter of 2.913 inches, ball diameter of 0.687 inches and ball number of 8. To achieve the ball-bearing fault frequencies regarding the inner ring fault, outer ring fault and ball fault, the formulas in (4), (5) and (6) are respectively used

$$f_{ir} = \frac{N_b}{2} f_r \left[1 + \frac{D_b}{D_c} cos(\theta)\right] \quad (4)$$

$$f_{or} = \frac{N_b}{2} f_r \left[1 - \frac{D_b}{D_c} cos(\theta)\right] \quad (5)$$

$$f_b = \frac{D_c}{D_b} f_r \left[1 - (\frac{D_b}{D_c} cos(\theta))^2\right] \quad (6)$$

where N_b is the number of balls, f_r is the motor rotational frequencies, θ is the ball contact angle, D_b is the ball diameter and D_c is the pitch diameter. Number of samples for each state is listed in Table. 1.

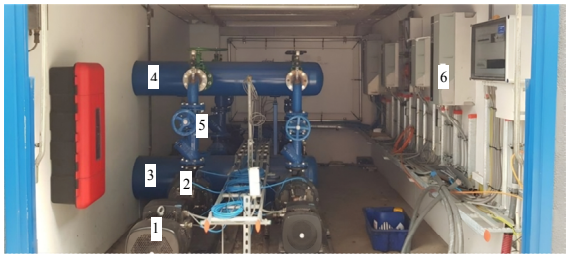

Fig. 6. The experimental set-up [24]: (1) electric motor; (2) pump; (3) main water inlet; (4) main water outlet; (5) discharge valve; and (6) variable frequency drive (vfd).

TABLE. 1. Dataset information

State	Number of samples
Outer Race Fault	270
Inner Race Fault	225
Ball Fault	90
Healthy	880

2.4. Feature Extraction & Selection

Extracting features from signal and select the most efficient features with the aim of removing useless information and dimensionality reduction, has a great impact on the performance, accuracy and training speed of the model. In this research, two signal processing techniques are used to extract features.

2.4.1. Time-Domain Features

First the Hilbert transform is applied on the raw signal in the time domain. By using the Hilbert transform, the envelope of the signal is obtained, which has the smoother shape than the raw signal. Also, this method removes high frequency components and large fluctuations from the signal. Thus, descriptive statistics such as the standard deviation, kurtosis and skewness are applied on the signal to extract features. The envelope of the signal in inner race fault, outer race fault and healthy state are shown in Fig. 7. The Hilbert transform, transforms the main signal into a complex signal, as follows:

$$z(t) = x(t) + jH[x(t)] \quad (7)$$

where $x(t)$ is the main signal, $H[x(t)]$ is the Hilbert transform of the main signal and can be calculated according to (8):

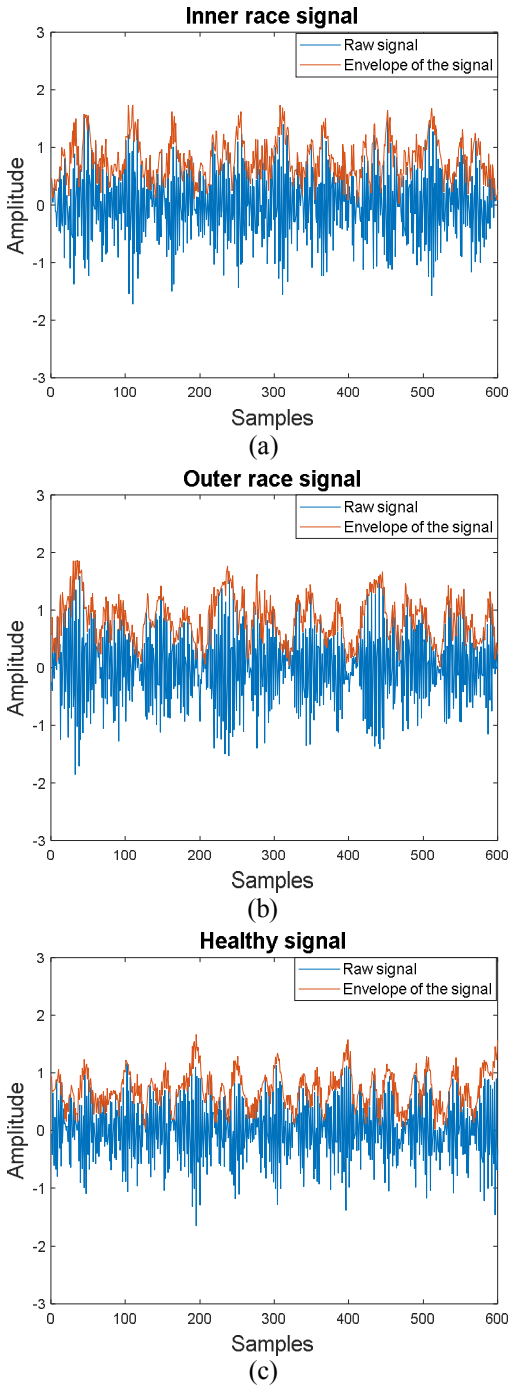

Fig. 7. The envelope for (a) inner race fault; (b) outer race fault, and (c) healthy signals.

$$H[x(t)] = \frac{1}{\pi}\int_{-\infty}^{+\infty}\frac{x(\tau)}{t-\tau}\,d\tau \tag{8}$$

The envelope of the signal can be calculated by taking the absolute value of $z(t)$

$$Envelope(t) = \sqrt{\{H[x(t)]\}^2 + \{x(t)\}^2} \tag{9}$$

2.4.2. Frequency-Domain Features

For features extraction in frequency domain, first, the envelope of the signal is transferred from time domain to frequency domain using PSD.

The signal regarding the ball fault, its envelope and their PSDs are shown in Fig. 8. According to this figure, after getting envelope and applying PSD, those frequencies that are not related to fault were removed or weakened and in the range of $f_{Fault} - 2 \leq f \leq f_{Fault} + 2$, descriptive statistical such as variance, root mean square and kurtosis are applied to frequency spectrum of the signal and extracted as the features in the frequency domain.

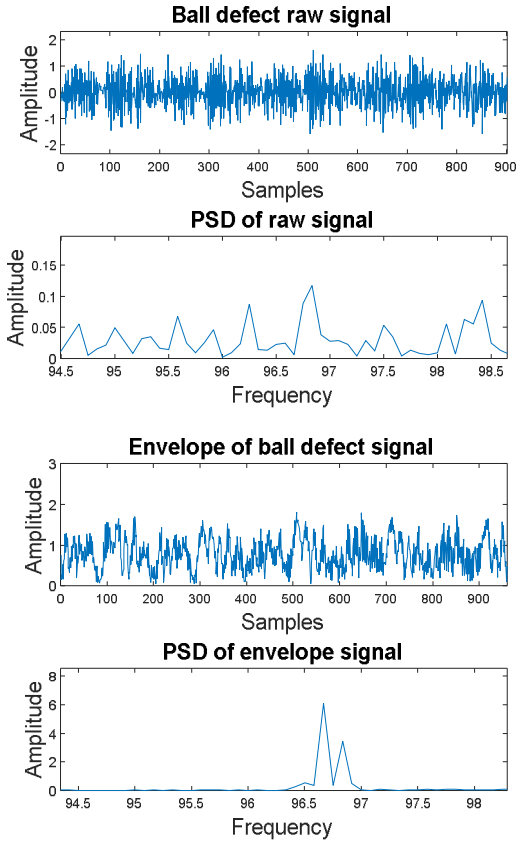

Fig. 8. (a) Ball Defect Raw Signal and Its Power Spectral Density; and (b) Envelope of the Ball Defect Signal and Its Power Spectral Density.

2.4.3. Feature Selection

Feature selection reduces complexity, over-fitting and also increase the performance and accuracy of the model by dimensionality reduction. Sequential feature selection is one of the feature selection techniques, which operates by selecting or removing features step by step and can be classified into two methods. In sequential forward feature selection, first, no feature is selected and at each step, feature that improves performance of the model is selected until no other feature increases the performance of the model. In sequential backward feature selection, first, all

the features all selected and the feature that has less impact on the model efficiency is removed until the removal of any remained feature reduces the model performance.

2.5. Models Evaluation

In this subsection, the performance of different algorithms on the dataset represented in [24] is examined. The confusion matrix for all the algorithms is shown in Figs. 7 and 8. The recall, precision, accuracy and F1-score techniques are used to evaluate each model performance. The mathematical formulas of these metrics are presented in (11) to (14):

$$Recall = \frac{TP}{TP + FN} \tag{11}$$

$$Precision = \frac{TP}{TP + FP} \tag{12}$$

$$F1 = 2 \times \frac{Precision \times Recall}{Precision + Recall} \tag{13}$$

$$Accuracy = \frac{TN + TP}{TP + FN + TN + FP} \tag{14}$$

where true positive (TP) is the number of faulty samples that are correctly predicted faulty, false positive (FP) is the number of healthy samples that are incorrectly predicted faulty, false negative (FN) is the number of faulty samples that are incorrectly predicted healthy and true negative (TN) is the number of healthy samples that are correctly predicted healthy. The evaluation results of the implemented algorithms are listed in Table. 2.

Fig. 9 shows the confusion matrices of different algorithms with the proposed procedure. Fig. 10 represents the confusion matrices for the conventional algorithms based on FFT, in which neither Hilbert transform nor PSD is used. Main diagonal entries of the matrix are samples that are correctly predicted and other entries demonstrate the incorrectly predicted samples. Among the four algorithms with the proposed procedure, the random forest method based on ensemble learning achieves the highest accuracy with 97.33%. Also, this model shows higher accuracy compared to those methods in which neither Hilbert transform nor PSD is used. The random forest model consists of 190 tree decision learners and AdaBoostM2 method is used. In the SVM model, one-vs.-all radial base function kernel is used for multi-class classification. The ANN structure is a feed-forward neural network, which is made of two hidden layers with 105 neurons for the first and 145 neurons for the second hidden layer. KNN algorithm with 2 neighbor and Manhattan distance is employed for the classification. The accuracies of the KNN, SVM and ANN are respectively 94.13%, 92.90% and 90.04%.

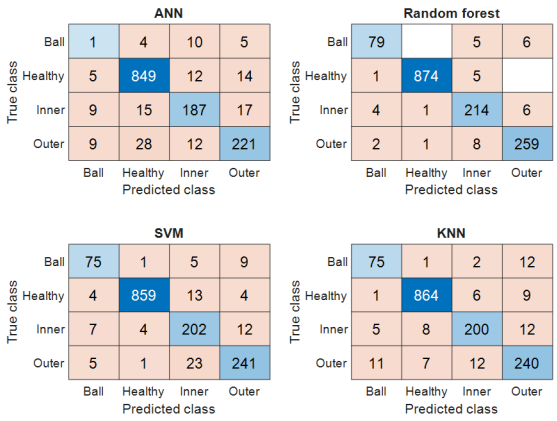

Fig. 9. Confusion matrices of the algorithms with the proposed procedure

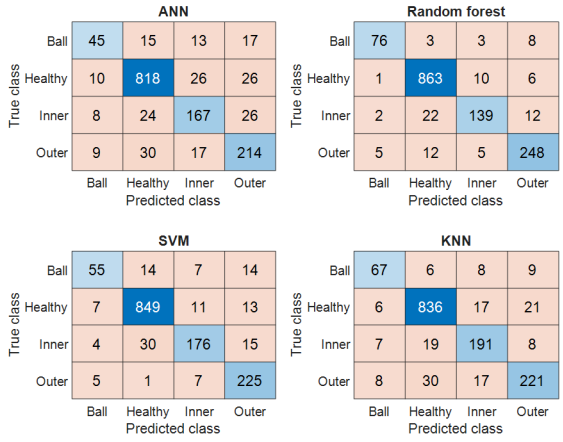

Fig. 10. Confusion matrix of the conventional algorithms without envelope and using FFT instead of PSD

Although SVM has less overall accuracy compared to KNN, according to Fig. 7, the number of misclassification for the inner race fault in SVM is less than that of KNN and the outer race fault is better predicted in SVM. The accuracies of the algorithms without using the Hilbert transform and PSD are shown in Table. 3.

TABLE. 2. Evaluation metrics for proposed model

Model	Precision	Accuracy	Recall	F1Score
ANN	%85.17	%90.04	%84.74	%84.93
KNN	%89.63	%94.13	%89.82	%89.72
SVM	%89.58	%92.90	%87.30	%88.35
RF	%94.86	%97.33	%94.53	%94.68

TABLE. 3. Comparative study on the accuracy for the proposed and conventional algorithms

Model	Non-Envelope and FFT	Envelope and PSD
ANN	%84.91	%90.04
KNN	%93.92	%94.13
SVM	%89.07	%92.90
RF	%93.92	%97.33

3. CONCLUSIONS

In this study, a ball-bearing fault detection method has been introduced using signal processing techniques and artificial intelligence algorithms. This method using Hilbert transform could remove high and unwanted frequencies and also weaken frequencies that are not related to ball-bearing fault. PSD is also used for better fault frequency detection and noise reduction for suitable feature extraction. Finally, the random forest method with the accuracy above 97% outperforms the other algorithms, i.e. SVM, KNN and ANN, in diagnosing ball-bearing fault.

REFERENCES

[1] G. R. Agah, A. Rahideh, H. Khodadadzadeh, S. M. Khoshnazar and S. Hedayati Kia, "Broken Rotor Bar and Rotor Eccentricity Fault Detection in Induction Motors Using a Combination of Discrete Wavelet Transform and Teager–Kaiser Energy Operator," *IEEE Transactions on Energy Conversion*, vol. 37, no. 3, pp. 2199-2206, Sep. 2022.

[2] G. R. Agah, A. Rahideh, V. Z. Faradonbeh and S. Hedayati Kia, "Stator Winding Inter-Turn Short-Circuit Fault Modeling and Detection of Squirrel-Cage Induction Motors," *IEEE Transactions on Transportation Electrification,* vol. 10, no. 3, pp. 5725-5734, Sep. 2024.

[3] A. Nasiri, A. Rahideh, G. R. Agah and S. H. Kia, "Ball-Bearing Fault Detection of Squirrel-Cage Induction Motors Based on Single-Phase Stator Current Using Wavelet Packet Decomposition and Statistical Features," *IEEE Transactions on Energy Conversion*, In Press 2024, DOI: 10.1109/TEC.2024.3461753.

[4] R. Alimardani, A. Rahideh and S. Hedayati Kia, "Mixed Eccentricity Fault Detection for Induction Motors Based on Time Synchronous Averaging of Vibration Signals," *IEEE Transactions on Industrial Electronics*, vol. 71, no. 3, pp. 3173-3181, March 2024.

[5] M. Aishwarya and R. M. Brisilla, "Design and Fault Diagnosis of Induction Motor Using ML-Based Algorithms for EV Application," *IEEE Access*, vol. 11, pp. 34186-34197, 2023.

[6] K. Yatsugi, S. E. Pandarakone, Y. Mizuno and H. Nakamura, "Common Diagnosis Approach to Three-Class Induction Motor Faults Using Stator Current Feature and Support Vector Machine," *IEEE Access*, vol. 11, pp. 24945-24952, 2023.

[7] M. Drakaki, L. Y. Karnavas, A. I. Tziafettas, V. Linardos and P. Tzionas, " Machine learning and deep learning based methods toward industry 4.0 predictive maintenance in induction motors: State of the art survey" *Industrial Engineering and Management*, vol. 15, no. 1, pp.31-57, 2021.

[8] J.-X. Liao *et al*., "BearingPGA-Net: A Lightweight and Deployable Bearing Fault Diagnosis Network via Decoupled Knowledge Distillation and FPGA Acceleration," *IEEE Transactions on Instrumentation and Measurement*, vol. 73, pp. 1-14, 2024.

[9] Y. Shu, W. Zhang, X. Song, G. Liu and Q. Jiang, "DBF-CNN: A Double-Branch Fusion Residual CNN for Diagnosis of Induction Motor Broken Rotor Bar," *IEEE Transactions on Instrumentation and Measurement*, vol. 72, pp. 1-10, 2023.

[10] J. Wang, L. Qiao, Y. Ye and Y. Chen, "Fractional envelope analysis for rolling element bearing weak fault feature extraction," *IEEE/CAA Journal of Automatica Sinica*, vol. 4, no. 2, pp. 353-360, April 2017.

[11] Z. Chen, Y. Yang, C. He, Y. Liu, X. Liu and Z. Cao, "Feature Extraction Based on Hierarchical Improved Envelope Spectrum Entropy for Rolling Bearing Fault Diagnosis," *IEEE Transactions on Instrumentation and Measurement*, vol. 72, pp. 1-12, 2023.

[12] Y. Yu, X. Zhao and C. Yu, "Wavelet-Based Time-Reassigned Synchroextracting Transform With Application to Fault Diagnosis of Flexible Thin-Wall Bearing," *IEEE Transactions on Instrumentation and Measurement*, vol. 72, pp. 1-12, 2023.

[13] R. Guo, Y. Wang, H. Zhang and G. Zhang, "Remaining Useful Life Prediction for Rolling Bearings Using EMD-RISI-LSTM," *IEEE Transactions on Instrumentation and Measurement*, vol. 70, pp. 1-12, 2021.

[14] H. Cui, Y. Guan and H. Chen, "Rolling Element Fault Diagnosis Based on VMD and Sensitivity MCKD," *IEEE Access*, vol. 9, pp. 120297-120308, 2021.

[15] F. Shen and R. Yan, "A New Intermediate-Domain SVM-Based Transfer Model for Rolling Bearing RUL Prediction," *IEEE/ASME Transactions on Mechatronics*, vol. 27, no. 3, pp. 1357-1369, June 2022.

[16] A. Biswas, S. Ray, D. Dey and S. Munshi, "Detection of Simultaneous Bearing Faults Fusing Cross Correlation With Multikernel SVM," *IEEE Sensors Journal*, vol. 23, no. 13, pp. 14418-14427, 1 July1, 2023.

[17] Z. -S. Syu and C. -H. Lee, "One-Dimensional Binary Convolutional Neural Network Accelerator Design for Bearing Fault Diagnosis," *IEEE Sensors Journal*, vol. 24, no. 3, pp. 3649-3658, 1 Feb.1, 2024.

[18] D. K. Supreeth, S. I. Bekinal and R. C. Shivamurthy, "Optimization of Radial Electrodynamic Bearing Using Artificial Neural Network," *IEEE Access*, vol. 12, pp. 67957-67970, 2024.

[19] J. Tian, C. Morillo, M. H. Azarian and M. Pecht, "Motor Bearing Fault Detection Using Spectral Kurtosis-Based Feature Extraction Coupled With K-Nearest Neighbor Distance Analysis," *IEEE Transactions on Industrial Electronics*, vol. 63, no. 3, pp. 1793-1803, March 2016.

[20] M. G. Alfarizi, J. Vatn and S. Yin, "An Extreme Gradient Boosting Aided Fault Diagnosis Approach: A Case Study of Fuse Test Bench," *IEEE Transactions on Artificial Intelligence*, vol. 4, no. 4, pp. 661-668, Aug. 2023.

[21] Z. Chen, J. Cen and J. Xiong, "Rolling Bearing Fault Diagnosis Using Time-Frequency Analysis and Deep Transfer Convolutional Neural Network," *IEEE Access*, vol. 8, pp. 150248-150261, 2020.

[22] B. Sun and X. Liu, "Significance Support Vector Machine for High-Speed Train Bearing Fault Diagnosis," *IEEE Sensors Journal*, vol. 23, no. 5, pp. 4638-4646, March, 2023.

[23] B. Wang, W. Qiu, X. Hu, and W. Wang, "A rolling bearing fault diagnosis technique based on recurrence quantification analysis and Bayesian optimization SVM," *Applied Soft Computing*, vol. 156, p. 111506, 2024.

[24] S. Bruinsma, R. D. Geertsma, R. Loendersloot, and T. Tinga, "Motor current and vibration monitoring dataset for various faults in an E-motor-driven centrifugal pump," *Data in Brief*, vol. 52, p. 109987, 2024.